THE JOURNAL OF PHYSICAL CHEMISTRY B

Article

pubs.acs.org/JPCB

Solvent Isotope Effect on the Dark Adaptation of Bacteriorhodopsin in Purple Membrane: Viewpoints of Kinetics and Thermodynamics

Han-Kuei Chiang and Li-Kang Chu*

Department of Chemistry, National Tsing Hua University, 101, Sec. 2, Kuang-Fu Rd., Hsinchu 30013, Taiwan

Supporting Information

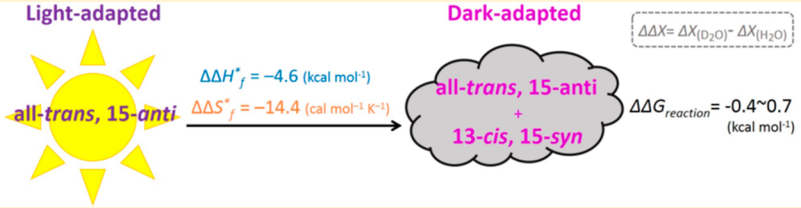

ABSTRACT: The thermal retinal isomerization from all-*trans*, 15-*anti* to 13-*cis*, 15-*syn* of bacteriorhodopsin in purple membrane in H_2O and D_2O during dark adaptation was investigated at 30−55 °C at neutral pH. In this temperature range, phase transition of purple membrane and destruction of the tertiary structure of bacteriorhodopsin did not take place. We found that the solvent isotope effect is inverted below about 45 °C; i.e., $k_f(D_2O)/k_f(H_2O) > 1$. Applying the transition state theory, the changes in enthalpy from the initial state to the transition state along the thermal *trans*-to-*cis* forward reaction coordinate, ΔH_f^*, were determined to be 24.7 ± 1.2 and 20.1 ± 0.4 kcal mol^{-1} in H_2O and D_2O, respectively. The relative entropic change of the transition state in H_2O and D_2O, $\Delta\Delta S_f^* = \Delta S_f^*(D_2O) - \Delta S_f^*(H_2O)$, was −14.4 ± 3.9 cal mol^{-1} K^{-1}. In addition, the Gibbs free energy of *trans*-to-*cis* thermal isomerization reaction in D_2O is 0.4−0.7 kcal mol^{-1} lower than that in H_2O. It is the first time the entropy and enthalpy of the transition state have been quantified to elucidate the solvent isotope effect in the retinal thermal isomerization of bacteriorhodopsin during dark adaptation. The solvent isotope effect on the thermodynamics properties and kinetics implied that the hydrogen bonding in the transition state during the dark adaptation of bR is stronger than that in the initial state.

1. INTRODUCTION

Bacteriorhodopsin (bR) is a transmembrane protein found in the halophile *Halobacterium salinarum*.[1] The hexagonal crystalline primitive units, containing three bR and nine lipids per bR, form the purple membrane (PM).[2,3] bR is mainly composed of seven α-helices and one retinal, which covalently links to Lys216 to form the protonated Schiff base.[4] At thermal equilibrium without illumination, the retinals in bR-PM possess two isomers: all-*trans*, 15-*anti* and 13-*cis*, 15-*syn* forms in the ratio of 1:1−1:2 at room temperature,[5−8] called dark adapted bR (bR_{DA}). Upon illumination, the constituent retinals become fully all-*trans*, which is called light-adapted bR (bR_{LA}). bR_{LA} exhibits photoactivity upon visible irradiation to pursue a photocycle in which two main processes take place, the retinal isomerization at C_{13}═C_{14} from all-*trans*, 15-*anti* to 13-*cis*, 15-*anti* and proton translocation in the bR interior.[9]

The transition from bR_{LA} to bR_{DA} in darkness involves the double isomerization of the retinal from the all-*trans*, 15-*anti* to 13-*cis*, 15-*syn*.[5−8] An early study showed slight changes in the enthalpy of 0.35 kcal mol^{-1} and in the entropy of 1.3 cal mol^{-1} K^{-1} for dark adaptation at room temperature.[7] Váró et al. determined the free energy change of retinal thermal *trans*-to-*cis* isomerization of bR-PM to be −0.36 kcal mol^{-1}.[10] These results suggested an equilibrium constant, $K = [cis]/[trans]$, of 1−2 at room temperature, consistent with the direction extraction of the retinal analyzed using high-performance liquid chromatography (HPLC).[5,8] In addition, theoretical works have been carried out to understand the energetics and the mechanism of the thermal isomerization process.[11,12] Baudry et al. reported that the free energy of the 13-*cis*, 15-*syn* retinal is 1.1 kcal mol^{-1} lower than that of the all-*trans* retinal.[11] Logunov and Schulten demonstrated that the isomerization process is catalyzed by the protonation of an aspartic acid (Asp85) and that a barrier of 22 kcal mol^{-1} exists along the *trans*-to-*cis* reaction coordinate.[12]

A number of studies have discussed the mechanisms of retinal isomerization during the dark adaptation of bR.[13−20] A fission of the hydrogen bond between the proton on Tyr185 and the carboxylate of Asp212 was proposed to lead to a free carboxylate of Asp212, which attacks the C_{13} on the retinal, causing nucleophilic catalysis in the *trans*-to-*cis* isomerization.[13−15] However, the NMR results did not show the evidence for tyrosinate in fully hydrated form during the dark adaption of bR at ambient or low temperature.[16] In addition, a three-dimensional crystalline structure study indicated that the displacement of the residues surrounding the Schiff base, Asp85, Thr89, and Leu93 is noticeably coupled with a slightly altered orientation in the moiety of the polyene train of the retinal and the surrounding residues, Trp86, Trp182, and

Received: December 20, 2013
Revised: February 9, 2014
Published: February 17, 2014

ACS Publications © 2014 American Chemical Society

dx.doi.org/10.1021/jp412475u | J. Phys. Chem. B 2014, 118, 2662−2669

Trp189, during the bR dark adaptation.[17] Moreover, a slight reduction in the bR volume, observed during the bR dark adaptation, indicated the formation of a few hydrogen bonds or the localized conformational change at the retinal moiety in the dark adaption of bR.[18−20] The solvent isotope effect on the rate of the thermal *trans*-to-*cis* isomerization exhibits an inverse isotope effect, k_D/k_H = 1.24, at 34 °C.[21] It also indicates less bounded proton(s) in the initial all-*trans* state than in the reactive intermediate prior to the rate controlling step of the retinal isomerization.

The thermal effect on miscellaneous biological functions and properties of bR and PM have been extensively studied, e.g., the thermochromism,[22] the light-induced photocycle kinetics,[23,24] the thermal stability and unfolding pathways of the tertiary structure of bR,[25−28] and the crystalline structure of PM.[29−33] However, less kinetics and thermodynamics information of the solvent isotope effect on the dark adaptation over a wide temperature range has been delivered. In this work, we investigated the kinetics and the thermodynamics properties of the transition of the thermal isomerization of the retinal from all-*trans*, 15-*anti* to 13-*cis*, 15-*syn* in H_2O and D_2O. Previous studies showed that the crystal structure of PM started to change at T > 60 °C, in association with altered activity of the circular dichroism, fluorescence intensity, and infrared spectroscopy.[29−32] The PM melted further and the tertiary structure of bR was further destroyed at 74−78 °C[33] and at T > 96 °C,[32] respectively. Under our experimental condition in the temperature range 30−55 °C, the configurations of PM and bR did not undergo permanent disruption. We found that the solvent isotope effect was inverted below 45 °C; i.e., $k_f(D_2O)/k_f(H_2O)$ > 1. Using the transition state theory to differentiate the contributions of entropy and enthalpy in the transition state during the bR-PM dark adaptation, we found that the enthalpy of the transition state along the *trans*-to-*cis* forward reaction coordinate, ΔH_f^*, in H_2O is 4.6 kcal mol^{-1} larger than that in D_2O. Moreover, the entropy change in the transition state with respect to the initial all-*trans* state in H_2O is 14.4 ± 3.9 cal mol^{-1} K^{-1} larger than that in D_2O. It implied that the strength of hydrogen bonding in the bR interior was altered during the dark adaptation.

2. MATERIALS AND METHODS

2.1. Materials Preparation. The preparation of PM fragments from the *H. salinarum* S9 strain followed a previous method.[34] The aqueous buffer solution at pH 7.4 was from Sigma-Aldrich. The D_2O-substituted buffer solution was prepared by drying a given amount of original H_2O-contained buffer, followed by re-adding the same amount of D_2O (Sigma-Aldrich) afterward. The PM in D_2O was prepared by redistributing the PM pellets into 0.6 mL of D_2O for 5 min, followed by centrifugation at 18 400*g* for 60 min. The above procedures were performed five times before the temperature-programmed experiments. The concentration of the bR_{LA}-PM was controlled at 6.4 μM.

2.2. Steady-State Spectroscopic Measurements. The bR-PM was light-adapted under illumination at room temperature prior to the steady-state absorption measurements. Visible absorption spectra were monitored with a spectrometer (USB4000−UV−VIS, Ocean Optics), and the temperature was controlled in the range 30−55 °C within a fluctuation of 0.01 °C at a set temperature using a thermostat (qpod TC125, Quantum Northwest) with a magnetic stirrer. A 0.8 mL portion of aqueous buffer solution was preheated in a 1 cm × 1 cm quartz cuvette at a given temperature for 10 min. Afterward, 200 μL of bR_{LA}-PM was added to the preheated solution. The final concentrations of buffer and bR_{LA}-PM were 0.1 mM and 6.4 μM, respectively. The cuvette was sealed thoroughly to prevent evaporation. The time-evolved steady-state absorption spectra at a set temperature were immediately collected in the darkness for a period of 4 h using an acquisition program, SpectraSuite. In addition, the circular dichroism (CD) spectra of the bR_{DA}-PM were recorded with a temperature-programmable spectrometer (model 410, AVIV) and averaged for 3 s at 1 nm intervals from 750 to 190 nm at 30 to 60 °C.

3. RESULTS

3.1. Steady-State Spectra. Steady-state visible spectroscopy was employed to determine the concentration of bR_{LA}-PM according to the intense absorption band at 568 nm attributed to the retinal moiety[35] and to differentiate the bR_{LA}-PM and bR_{DA}-PM, which is characterized at 559 nm.[8] Circular dichroism (CD) spectroscopy was used to confirm the integrity of the bR trimers in the PM according to a characteristic biphasic lobe in the spectral range 450−600 nm, ascribed to the exciton coupling among the retinals in bR trimer in PM.[36]

3.1.1. Absorption Spectra in Visible Region. The visible absorption spectra of bR_{LA}-PM in H_2O and D_2O at 22 °C are shown in Figure S1 in the Supporting Information. The identical contours imply that changing the solvent from H_2O to D_2O does not alter the electronic transition of the protonated retinal Schiff base, so the absorption contour is preserved. The normalized visible absorption contours of the retinal moiety of bR_{LA}-PM after 1 h of dark adaptation in H_2O and D_2O in a temperature range of 30−55 °C exhibited a significant blueshift, shown in parts a and b of Figure 1, respectively. The band at 568 nm, attributed to the all-*trans* retinal in bR_{LA}-PM, gradually shifted to 560 nm; this is attributed to the bR_{DA}-PM, which is composed of the mixture of *trans* (λ_m = 568 nm) and *cis* (λ_m = 555 nm) retinals.[8] The higher the temperature was, the more blueshifted was the absorption contour for the same period of dark adaptation. This trend indicated that the transition from the bR_{LA}-PM to bR_{DA}-PM was apparently accelerated as the temperature was increased in both D_2O and H_2O. The kinetics and thermodynamics properties of the dark adaptation of bR-PM can be quantitatively determined by measuring the time-evolved absorption spectra at different temperatures. In order to avoid the contribution from the phase transition of PM and destruction of the tertiary structure of bR that occurred at T > 70 °C,[8,37] the temperature-programmed measurements were performed below 55 °C.

3.1.2. CD Spectra. Because the CD spectrometer was operated in dispersive scan mode, it was not easy to maintain the bR_{LA}-PM during the wavelength scanning in the measurements. Therefore, we collected the CD spectra of the bR_{DA}-PM at different temperatures. The CD spectra of the retinal moiety in H_2O and D_2O at 30−60 °C are shown in parts a and b of Figure 2, respectively. The characteristic biphasic lobes remained unchanged at 30−50 °C, with slight reduction in the ellipticity at 60 °C, whether the bR_{DA}-PM was in H_2O or D_2O, indicating that there was no significant destruction of the bR and PM. This finding is consistent with a previous result that the phase transition of PM takes place at T > 60 °C, leading to the depletion of the biphasic ellipticity and the generation of the monophasic lobe.[29] We therefore confirmed that the alteration of the kinetics of the bR-PM light-to-dark adaptation at varied temperatures below 60 °C was not due to the alteration of the trimeric

dx.doi.org/10.1021/jp412475u | J. Phys. Chem. B 2014, 118, 2662−2669

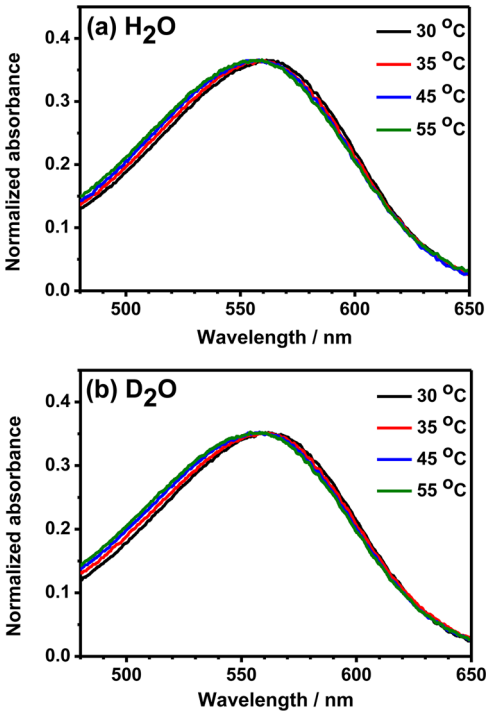

Figure 1. The normalized temperature-dependent steady-state absorption spectra of bR in (a) H_2O and (b) D_2O in the temperature range 30−55 °C after 1 h of dark-adaption at the given temperatures. The concentrations of constituent bR-PM were controlled at 6.4 μM, dispersed in 0.1 mM phosphate buffer.

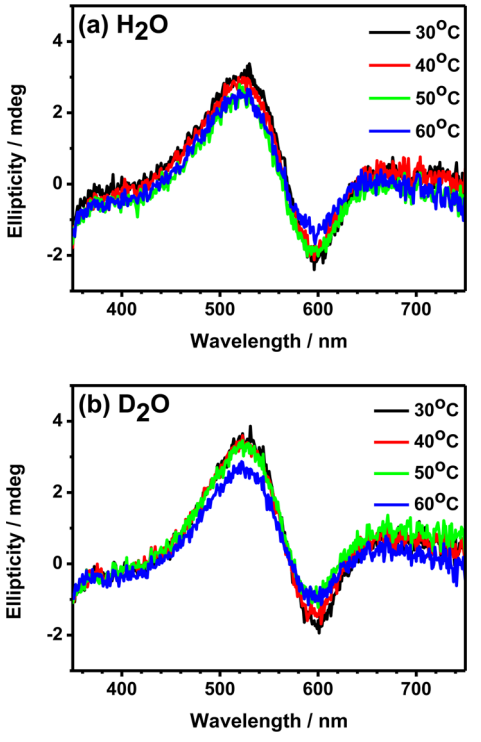

Figure 2. The steady-state circular dichroism spectra in 350−750 nm of PM in (a) H_2O and (b) D_2O in the temperature range 30−60 °C. The concentrations of bR_{DA}-PM were controlled at 6.4 μM, dispersed in 0.1 mM phosphate buffer.

configuration of bR-PM and the denaturing of the tertiary structure of bR.

3.2. Time-Evolved Visible Difference Spectra in the Temperature Range 30−55 °C. In section 3.1.1, we observed the thermal isomerization of the all-*trans* retinal in bR_{LA}-PM during dark adaptation according to the blueshift of the absorption contour of the retinal moiety from 568 to 560 nm. The temporally evolved absorption contours of bR-PM were collected to investigate the kinetics of the all-*trans* retinal thermal isomerization upon increases in temperature without the phase transition of the PM at $T < 60$ °C. The evolution of the difference spectra, $\Delta A(t)$, with respect to the absorption spectrum at time zero, $A(0)$, of bR_{LA}-PM in H_2O and D_2O at 50 °C are shown in parts a and b of Figure 3, respectively. The corresponding

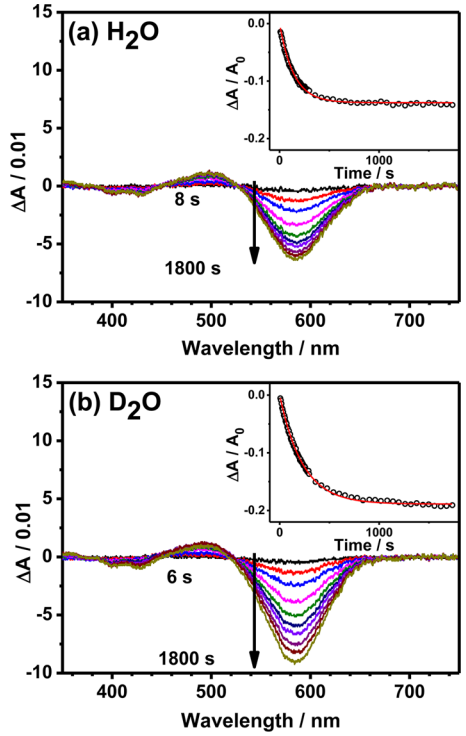

Figure 3. The time-evolved difference spectra of PM in (a) H_2O and (b) D_2O at 50 °C. The corresponding transformation evolution, $\Phi(t)$, at 568 nm is shown in the inset. The dots and solid lines represent the observed and fitted data (using eq 7), respectively.

transformation evolution, $\Phi(t)$, denoted as the ratio of $\Delta A(t)/A(0)$, at 568 nm is shown as the circles in the insets of Figure 3. The difference spectra and transformation evolutions obtained from the identical experiments performed in a temperature range of 30−55 °C in H_2O and D_2O are also shown in parts a and b of Figures S2 in the Supporting Information, respectively. We found that the absorbance at 568 nm was gradually depleted, followed by the generation at approximately 500 nm. An isosbestic point appeared at 524 nm in both H_2O and D_2O, referring to the linearly stoichiometric relationship between these two components at 568 and 500 nm. Comparing with the thermal effect on rhodopsin, both thermal isomerization and hydrolysis of the Schiff base retinal occurred when the temperature was up to about 56 °C.[38,39] The hydrolyzed retinal was characterized at approximately 380 nm.[39−41] In contrast with rhodopsin, no increase in the absorbance at 380 nm was observed in the evolution of difference spectra of bR_{LA}-PM at 50 °C, as shown in Figure 3. In addition, the evolutions of the absorbance difference at 568 and 380 nm at 55 °C, shown in the Supporting

dx.doi.org/10.1021/jp412475u | J. Phys. Chem. B 2014, 118, 2662−2669

Information (Figure S3), did not change with time. As a result, the thermal hydrolysis of bR-PM was excluded when the temperature varied in the 30−55 °C range and thermal isomerization of the retinal was solely taken into consideration in the kinetics modeling.

In a similar manner, the transformation evolution decreased rapidly in the early stage and became stable in the later stage. Although the apparent rate coefficient has been employed to investigate the kinetics of the dark adaptation of bR_{LA}-PM previously,[10,21] the correlative thermodynamics properties of the *trans*-to-*cis* reaction were not properly determined because the apparent rate coefficient included the contributions from the forward and reversed reactions. As a result, we introduce a reversible kinetics model, coupled with well-defined mathematical expression, to properly describe the temporal behavior of the optical modulation at a given wavelength during the dark adaptation of the bR_{LA}-PM

$$trans \underset{k_r}{\overset{k_f}{\rightleftarrows}} cis, \quad \text{with initial concentration } [trans] = [trans]_0 \text{ and } [cis] = 0 \tag{1}$$

where k_f and k_r represent the rate coefficients of the forward and reverse reactions, respectively. Solving the differential equation on the basis of eq 1, the evolutions of the *trans* and *cis* retinals are determined in the following forms:

$$[trans]_t = \frac{[trans]_0}{k_f + k_r}(k_r + k_f e^{-(k_f+k_r)t}) \tag{2a}$$

$$[cis]_t = \frac{k_f[trans]_0}{k_f + k_r}(1 - e^{-(k_f+k_r)t}) \tag{2b}$$

At a given wavelength λ at time zero, the absorbance is proportional to the initial concentration of *trans* retinal

$$A_\lambda(0) = \theta_\lambda \times b \times [trans]_0 \tag{3}$$

where θ_λ and b represent the extinction coefficient of *trans* retinal at a given wavelength λ and the absorption path length of the cuvette, respectively. At time > 0, the evolution of the absorbance at a given wavelength λ is composed of the $[trans]_t$ and $[cis]_t$

$$A_\lambda(t) = \theta_\lambda \times b \times [trans]_t + \varphi_\lambda \times b \times [cis]_t = \frac{b \times [trans]_0}{k_f + k_r}[(\theta_\lambda k_r + \varphi_\lambda k_f) + k_f(\theta_\lambda - \varphi_\lambda)e^{-(k_f+k_r)t}] \tag{4}$$

where φ_λ represents the extinction coefficient of *cis* retinal at a given wavelength λ. The evolution of the absorbance difference at a given wavelength λ, $\Delta A_\lambda(t) = A_\lambda(t) - A_\lambda(0)$, can be expressed as

$$\Delta A_\lambda(t) = A_\lambda(t) - A_\lambda(0) = \frac{b \times [trans]_0 \times k_f \times (\varphi_\lambda - \theta_\lambda)}{k_f + k_r}(1 - e^{-(k_f+k_r)t}) \tag{5}$$

We defined the transformation evolution, $\Phi(t)$, as the relative absorbance difference modulation with respect to $A_\lambda(0)$:

$$\Phi(t) = \frac{\Delta A_\lambda(t)}{A_\lambda(0)} = \frac{(\varphi_\lambda - \theta_\lambda) \times k_f}{(k_f + k_r) \times \theta_\lambda} \times (1 - e^{-(k_f+k_r)t}) \tag{6}$$

Using $y = m \times (1 - e^{-nt})$ (eq 7) to fit the observed $\Phi(t)$, as shown in the solid lines in the insets of Figures 3 and S2 (Supporting Information), the parameters n and m can be obtained and listed in Table 1. n and m are equivalent to the following terms:

$$n = k_f + k_r, \quad m = \frac{(\varphi_\lambda - \theta_\lambda) \times k_f}{(k_f + k_r) \times \theta_\lambda} \tag{7}$$

Table 1. The Parameters, *m* and *n*, Derived from the Fitting of Transformation Evolutions, $\Phi(t)$, at 568 nm in the Temperature Range 30−55 °C in H_2O and D_2O Using eq 7

	H_2O		D_2O	
temperature (°C)	$m/10^{-1}$ (unitless)	$n/10^{-3}$ (s^{-1})	$m/10^{-1}$ (unitless)	$n/10^{-3}$ (s^{-1})
30	−1.31	0.5	−1.60	0.6
35	−1.27	1.2	−1.93	0.9
40	−1.32	2.3	−1.98	1.5
45	−1.44	3.7	−1.78	2.8
50	−1.38	7.0	−1.89	4.3
55	−1.58	9.6	−1.93	6.7

The product of m and n is expressed in the following form:

$$n \times m = \frac{(\varphi_\lambda - \theta_\lambda)}{\theta_\lambda} \times k_f \tag{8}$$

which is proportional to k_f. In order to derive the thermodynamics properties of the *trans*-to-*cis* thermal isomerization of the retinal in bR-PM, the rate coefficient k_f can be expressed in the following term using the transition state theory

$$k_f = \frac{k_B T}{h} e^{\Delta S_f^*/k_B} e^{-\Delta H_f^*/k_B T} \tag{9}$$

where k_B and h represent the Boltzmann constant and Planck constant, respectively. ΔS_f^* and ΔH_f^* denote the entropy and enthalpy changes from the initial state to the transition state, respectively, for the forward reaction. Thus, ΔH_f^* can be determined using the Eyring−Polanyi plot

$$\ln\left(\frac{|n \times m|}{T}\right) = \frac{-\Delta H_f^*}{k_B}\frac{1}{T} + \ln\left(\frac{k_B}{h}\right) + \frac{\Delta S_f^*}{k_B} + \ln\left(\left|\frac{\varphi_\lambda - \theta_\lambda}{\theta_\lambda}\right|\right) \tag{10}$$

Plotting $\ln(|n \times m|/T)$ versus T^{-1}, as shown in Figure 4b, $-\Delta H_f^*/k_B$ is determined from the slope, and the intercept is $\ln(k_B/h) + (\Delta S_f^*/k_B) + \ln(|(\varphi_\lambda - \theta_\lambda)/\theta_\lambda|)$.

In addition, the equilibrium constant can also be derived from $1/m$ at a given temperature

$$\frac{1}{m} = \frac{\theta_\lambda}{\varphi_\lambda - \theta_\lambda} \times \left(1 + \frac{k_r}{k_f}\right) = \frac{\theta_\lambda}{\varphi_\lambda - \theta_\lambda} \times \left(1 + \frac{1}{K}\right) \quad \text{where} \quad K = \frac{k_f}{k_r} = \frac{[cis(\infty)]}{[trans(\infty)]} \tag{11}$$

and

$$\Delta G = -RT \ln K \tag{12}$$

ΔG represents the change of Gibbs free energy of thermal isomerization of the retinal during the dark adaptation.

dx.doi.org/10.1021/jp412475u | J. Phys. Chem. B 2014, 118, 2662−2669

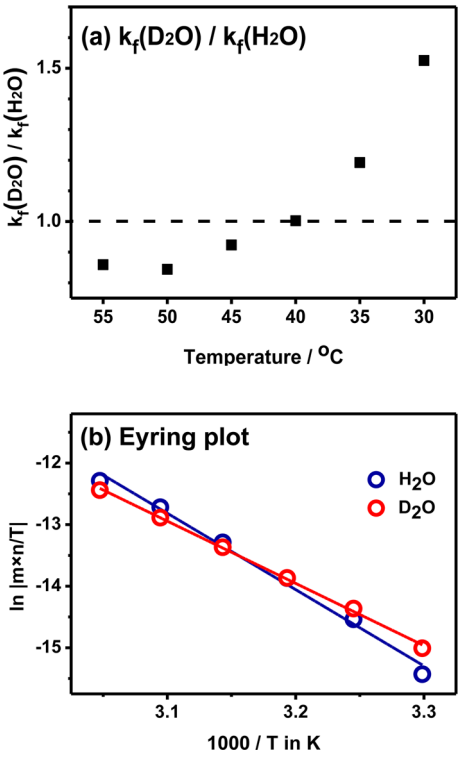

Figure 4. (a) The ratios of forward rate constants in H_2O and D_2O, $k_f(D_2O)/k_f(H_2O)$, at different temperatures. (b) Plots of $\ln(|n \times m|/T)$ with respect to the reciprocal of temperature in H_2O (blue) and D_2O (red) in the temperature range 30−55 °C. The open circles and solid lines represent the observed and fitted data (using eq 10), respectively.

4. DISCUSSION

4.1. Solvent Isotope Effect in Kinetics of the Dark Adaptation. Seltzer observed an inverted solvent isotope effect, $k_f(D_2O)/k_f(H_2O) = 1.24$, in the *trans*-to-*cis* retinal isomerization during the dark adaptation of bR_{LA}-PM at 34 °C.[21] In comparison with our observed ratios of $k_f(D_2O)/k_f(H_2O)$ in the temperature range 30−55 °C, as plotted in Figure 4a, an inverted isotope effect, $k_f(D_2O)/k_f(H_2O) = 1.19$, at 35 °C was consistent with Seltzer's report. However, if the temperature rises higher than 45 °C, the isotope effect will not be inverted. In comparison with rhodopsin, a normal solvent isotope effect, $k_f(D_2O)/k_f(H_2O) = 0.66$, was observed in the thermal retinal isomerization from 11-*cis* to all-*trans* at 59 °C, as reported by Yan et al.[38] Our result was similar to that reported value. This finding indicated that temperature played a role in the isotope effect for the retinal thermal isomerization. However, the corresponding thermodynamic properties, such as entropy and enthalpy, during the dark adaptation of bR_{LA}-PM in different isotope-substituted solvents have not been thoroughly discussed.

Previous theoretical studies have shown that the photoisomerization energy barrier of the protonated Schiff base retinal in light-adapted bR from all-*trans*, 15-*anti* to 13-*cis*, 15-*anti* along the ground-state potential energy surface was determined to be 24−29 kcal mol^{-1}.[42−44] The barrier height is closely correlated to the types of motions at C_{13}═C_{14}, such as hula-twist, one bond rotation, and bicycle pedal, and the charged distribution in the vicinity of retinal.[14] In the dark adaptation of bR_{LA}-PM, the barrier height of the retinal isomerization from all-*trans*, 15-*anti* to 13-*cis*, 15-*syn* was experimentally determined as 26−27 kcal mol^{-1},[8,15] and a higher value of 31 kcal mol^{-1} was determined with high-pressure near-infrared Raman spectroscopy.[19] In rhodopsin, the protonated Schiff base retinal isomerization from 11-*cis* to *all-trans* exhibits a barrier at about 26 kcal mol^{-1} along the ground state potential energy surface.[45] In this work, we obtained that the enthalpic difference between the initial state and the transition state, $\Delta H_f^*(H_2O)$, during the dark adaptation of bR_{LA}-PM in H_2O is 24.7 ± 1.2 kcal mol^{-1}, which agrees with most previously reported values. When the solvent is changed to D_2O, however, we found a reduced $\Delta H_f^*(D_2O)$ of 20.1 ± 0.4 kcal mol^{-1}. Moreover, the decrease in entropy change from H_2O to D_2O, $\Delta\Delta S_f^* = \Delta S_f^*(D_2O) - \Delta S_f^*(H_2O)$, was −14.4 ± 3.9 cal mol^{-1} K^{-1}. The corresponding thermodynamics properties are also summarized in Table 2.

Table 2. The Thermodynamics Properties of the All-*trans*, 15-*anti* to 13-*cis*, 15-*syn* Retinal Isomerization during the Dark Adaptation of bR-PM in H_2O and D_2O[a]

	H_2O		D_2O
ΔH_f^* (kcal mol^{-1})	24.7 ± 1.2		20.1 ± 0.4
$\Delta\Delta H_f^*$ (kcal mol^{-1})		−4.6 ± 1.2	
$\Delta\Delta S_f^*$ (cal mol^{-1} K^{-1})		−14.4 ± 3.9	
$\Delta G^0_{reaction}$ (kcal mol^{-1})	0 to −0.4		−0.4 to −1.1

[a] $\Delta\Delta H_f^* = \Delta H_f^*(D_2O) - \Delta H_f^*(H_2O)$; $\Delta\Delta S_f^* = \Delta S_f^*(D_2O) - \Delta S_f^*(H_2O)$.

Seltzer demonstrated that hydrogen bonds in bR_{LA}-PM are less bounded than that in the reactive intermediate prior to the rate controlling step of the retinal isomerization.[21] Accounting for the zero point energy in the transition state, it was reasonable that our measurements detected a reduction in the enthalpy of the transition in the transfer from H_2O to D_2O. According to the report by Makhatadze et al., the enthalpy change is decreased in the protein unfolding process when the solvent transfers from H_2O to D_2O, involving the exposure of the nonpolar group buried in the interior of the protein to the solvent.[46] Therefore, as the H_2O was substituted by D_2O, the interior environment of the bR cavity in the transition state was altered, probably in association with the exposure of the interior residues to D_2O, leading to a decrease in the enthalpy. Moreover, we observed a decrease in the entropy change from H_2O to D_2O. It is difficult to specifically ascribe our macroscopic observation to a single reason and to quantitatively determine the alteration of the strength of the hydrogen bonding during the dark adaptation of retinal because the visible spectra were not capable of reflecting the content of the water in the bR interior. Makhatadze and Privalov have demonstrated that hydrogen bonding, hydrophobic interaction, van der Waals force, and alteration of the protein configuration could lead to changes in the enthalpy, entropy, and heat capacity.[47] Although many probable mechanisms have been proposed, mainly involving nucleophilic catalysis,[13−15] we do not address this topic here with excessive description beyond our experimental evidence because the obtained thermodynamics properties denoted the ensemble of the hydrogen bonding network. We concluded that the great enthalpic and entropic differences in the transition states in H_2O and D_2O could likely be attributed to the hydrophobicity of the bacterioopsin moiety and the strength of the localized hydrogen bonding in the vicinity of the Schiff base. Although parts of the constituent residues, such as arginines, lysines, aspartic acids, glutamic acids, threonines, tyrosines, and tryptophans, were readily H/D exchangeable, further theoretical investigations, specific mutagenesis,[48] and temperature-programmable infrared spectroscopy[49] might help to unravel the alteration of the

dx.doi.org/10.1021/jp412475u | J. Phys. Chem. B 2014, 118, 2662−2669

hydrogen bonds, residues in the retinal vicinity, and the corresponding energetics in thermal retinal isomerization of bacteriorhodopsin at the molecular level. The molecular dynamics simulation might also be performed to narrow down the candidate residue(s) and its/their concomitant water networks resulting in the kinetic isotope effect. By means of infrared spectroscopy, the alteration of hydrogen bond strengths between bR and water can be unraveled upon analyzing the hydrogen-bonding sensitive bands: amide A (3300 cm^{-1}) and amide I (1660 cm^{-1}) bands of bR, attributed to the N—H stretch and C═O stretch,[50,51] and a broad continuum in the 1500−2000 cm^{-1} range, attributed to the bending vibrational modes of protonated water clusters.[52,53]

4.2. Isotope Effect in the Heat of Reaction. The transformation evolution at $t = \infty$, $\Phi(\infty) = \Delta A_\lambda(t = \infty)/A_\lambda(0)$, approaches the term m, which is a function of the equilibrium constant derived in eq 11. We observed an intrinsic difference of m in D_2O and H_2O, listed in Table 1, and therefore claimed an isotope effect in the equilibrium constant. Previous studies have shown that the ratio of the population of *cis* to *trans* retinal at equilibrium at approximately room temperature is about 1−2,[5−8] which implies that the upper limit of the Gibbs free energy change of the thermal *trans*-to-*cis* reaction in H_2O is only −0.4 kcal mol^{-1}. Under our experimental condition of 30−55 °C, the equilibrium constant K varied from 1.94 to 1.85 using the above-mentioned Gibbs free energy. The equilibrium K can be reasonably treated as unchanged in the temperature range 30−55 °C and can be averaged as 1.9. The observed $1/m$ in H_2O experiments, which is proportional to $(1 + (1/K))$ in eq 11, seemed to be unchanged and exhibited an average value of 7.2 within 5% variation. Using $K_{H_2O} = 1.9$, $\theta_\lambda/(\varphi_\lambda - \theta_\lambda)$ is accordingly determined as 4.7. According to the absorption spectra of light-adapted bR in H_2O and D_2O at 22 °C in Figure S1 (Supporting Information), the absorption contours were identical in H_2O and D_2O. As a result, it is reasonable to assume that the ratio $\theta_\lambda/(\varphi_\lambda - \theta_\lambda)$ is identical in D_2O and H_2O at a given wavelength λ. Comparing the averaged value of $1/m$, about 5.4 in D_2O experiments, the upper limit of K_{D_2O} was determined to be 6.7 using $\theta_\lambda/(\varphi_\lambda - \theta_\lambda) = 4.7$, equivalent to a Gibbs free energy change of reaction of −1.1 kcal mol^{-1} at room temperature. In contrast, using $K_{H_2O} = 1$ and doing a similar calculation, $\theta_\lambda/(\varphi_\lambda - \theta_\lambda)$ is 3.6 and K_{D_2O} is 2.0, equivalent to a Gibbs free energy change of reaction of −0.4 kcal mol^{-1}. Therefore, we can estimate that the free energy of the *trans*-to-*cis* isomerization during the dark adaptation of bR_{LA}-PM is lowered by 0.4−0.7 kcal mol^{-1} if the solvent is changed from H_2O to D_2O. However, our observation disagrees with previous studies on the solvent isotope effect in the equilibrium constant of the [*trans*]/[*cis*] for bR_{DA}-PM.[21]

Seltzer demonstrated that the isotope effects on the forward and reverse rate coefficients of dark adaptation are approximately equal to each other.[21] This conclusion implied that the Gibbs free energy of the reaction was not altered by changing the solvent from H_2O to D_2O. The ratio of all-*trans* to 13-*cis* retinal in bR_{DA}-PM was determined using hydroxylamine (NH_2OH:bR = 10^5:1) to convert the chromophores to the oximes and analyzing the mixture by HPLC.[21] However, the process becomes accessible when the bR/hydroxylamine mixture is illuminated with dim red light[54] or broadband light, and the intermediate M was regarded as the precursor to react with hydroxylamine.[55] As a result, the population of *cis* retinal might be underestimated because the illumination is able to drive *cis* retinal to *trans*, in terms of the light-adapted form.

As mentioned previously, the hydrogen bonding, hydrophobic interaction, and alteration of the protein configuration could lead to changes in the enthalpy, entropy, and Gibbs free energy during the transformation of the protein structure.[47] Using our detection method, proposed mechanism, and corresponding formula, we were able to quantify those macroscopic thermodynamic properties.

5. CONCLUSIONS

Using steady-state absorption spectroscopy in the visible region, the solvent isotope effect in the thermal isomerization of the retinal from all-*trans*, 15-*anti* to 13-*cis*, 15-*syn* during the dark adaptation of bR_{LA}-PM was investigated in H_2O and D_2O at 30−55 °C at neutral pH. In this temperature region, the purple membrane reserved its trimeric configuration and the tertiary structure of bacteriorhodopsin did not undergo destruction. Employing the transition state theory, we determined that the changes in enthalpy between the initial state and the transition state along the *trans*-to-*cis* forward reaction coordinate, ΔH_f^*, were 24.7 ± 1.2 and 20.1 ± 0.4 kcal mol^{-1} in H_2O and D_2O, respectively. The relative entropy change of the transition state in H_2O and D_2O, $\Delta\Delta S_f^* = \Delta S_f^*(D_2O) - \Delta S_f^*(H_2O)$, was 14.4 ± 3.9 cal mol^{-1} K^{-1}. In addition, the free energy of the *trans*-to-*cis* thermal isomerization in D_2O was 0.4−0.7 kcal mol^{-1} lower than that in H_2O. The solvent isotope effect on the dark adaptation kinetics and the thermodynamics properties implied that the strength of hydrogen bonding and the hydrophobicity in the bR interior were altered in D_2O. This finding suggests the need for further theoretical studies to elucidate the roles of isotope-substituted solvent in altering the thermodynamics properties of the dark adaptation of the bacteriorhodopsin.

■ ASSOCIATED CONTENT

Supporting Information

Figures showing steady-state absorption spectra, time-evolved difference spectra, and evolutions of the absorbance difference. This material is available free of charge via the Internet at http://pubs.acs.org.

■ AUTHOR INFORMATION

Corresponding Author

*Phone: +886-3-5715131, ext. 33396. Fax: +886-3-5711082. E-mail: lkchu@mx.nthu.edu.tw.

Notes

The authors declare no competing financial interest.

■ ACKNOWLEDGMENTS

This work is supported by National Science Council of Taiwan (NSC 101-2113-M-007-016-MY2) and Ministry of Education of R. O. C. (Grant No. 101N2011E1).

■ ABBREVIATIONS

bR, bacteriorhodopsin; PM, purple membrane; bR_{DA}, dark-adapted bacteriorhodopsin; bR_{LA}, light-adapted bacteriorhodopsin; bR-PM, bR purple membrane; bR_{DA}-PM, dark-adapted bR purple membrane; bR_{LA}-PM, light-adapted bR purple membrane

■ REFERENCES

(1) Oesterhelt, D.; Stoeckenius, W. Rhodopsin-Like Protein from Purple Membrane of Halobacterium halobium. *Nature New Biol.* **1971**, *233*, 149−152.

(2) Cartailler, J.-P.; Luecke, H. X-ray Crystallographic Analysis of Lipid-Protein Interactions in the Bacteriorhodopsin Purple Membrane. *Annu. Rev. Biophys. Biomol. Struct.* **2003**, *32*, 285−310.
(3) Dracheva, S.; Bose, S.; Hendler, R. W. Chemical and Functional Studies on the Importance of Purple Membrane Lipids in Bacteriorhodopsin Photocycle Behavior. *FEBS Lett.* **1996**, *382*, 209−212.
(4) Luecke, H.; Schobert, B.; Richter, H.-T.; Cartailler, J.-P.; Lanyi, J. K. Structure of Bacteriorhodopsin at 1.55 Å Resolution. *J. Mol. Biol.* **1999**, *291*, 899−911.
(5) Maeda, A.; Iwasa, T.; Yoshizawa, T. Isomeric Composition of Retinal Chromophore in Dark-adapted Bacteriorhodopsin. *J. Biochem.* **1977**, *82*, 1599−1604.
(6) Stoeckenius, W.; Lozier, R. H.; Bogomolni, R. A. Bacteriorhodopsin and the Purple Membrane of Halobacteria. *Biochim. Biophys. Acta* **1979**, *505*, 215−278.
(7) Sperling, W.; Carl, P.; Rafferty, Ch. N.; Dencher, N. A. Photochemistry and Dark Equilibrium of Retinal Isomers and Bacteriorhodopsin Isomers. *Biophys. Struct. Mech.* **1977**, *3*, 79−94.
(8) Scherrer, P.; Mathew, M. K.; Sperling, W.; Stoeckenius, W. Retinal Isomer Ratio in Dark-Adapted Purple Membrane and Bacteriorhodopsin Monomers. *Biochemistry* **1989**, *28*, 829−834.
(9) Lanyi, J. K. Molecular Mechanism of Ion Transport in Bacteriorhodopsin: Insights from Crystallographic, Spectroscopic, Kinetic, and Mutational Studies. *J. Phys. Chem. B* **2000**, *104*, 11441−11448.
(10) Kovács, I.; Hollós-Nagy, K.; Váró, G. Dark Adaptation and Spectral Changes in Triton-X-100-treated Bacteriorhodopsin. *J. Photochem. Photobiol. B* **1995**, *27*, 21−25.
(11) Baudry, J.; Crouzy, S.; Roux, B.; Smith, J. C. Simulation Analysis of the Retinal Conformational Equilibrium in Dark-Adapted Bacteriorhodopsin. *Biophys. J.* **1999**, *76*, 1909−1917.
(12) Logunov, I.; Schulten, K. Quantum Chemistry: Molecular Dynamics Study of the Dark-Adaptation Process in Bacteriorhodopsin. *J. Am. Chem. Soc.* **1996**, *118*, 9727−9735.
(13) Seltzer, S.; Zuckermann, R. Dynamic *Cis-Trans* Isomerization of Retinal in Dark-Adapted Bacteriorhodopsin. *J. Am. Chem. Soc.* **1985**, *107*, 5523−5525.
(14) Seltzer, S. MNDO Barrier Heights for Catalyzed Bicycle-Pedal, Hula-Twist, and Ordinary *Cis-Trans* Isomerizations of Protonated Retinal Schiff Base. *J. Am. Chem. Soc.* **1987**, *109*, 1627−1631.
(15) Birnbaum, D.; Seltzer, S. The Secondary β-Deuterium Isotope Effect in Dark Adaptation of Bacteriorhodopsin Containing Retinal-20,20,20-d_3. *Bioorg. Chem.* **1991**, *19*, 18−28.
(16) Herzfeld, J.; Das Gupta, S. K.; Farrar, M. R.; Harbison, G. S.; McDermott, A. E.; Pelletier, S. L.; Raleigh, D. P.; Smith, S. O.; Winkel, C.; Lugtenberg, J.; Griffin, R. G. Solid-State ^{13}C NMR Study of Tyrosine Protonation in Dark-Adapted Bacteriorhodopsin. *Biochemistry* **1990**, *29*, 5567−5574.
(17) Nishikawa, T.; Murakami, M.; Kouyama, T. Crystal Structure of the 13-*cis* Isomer of Bacteriorhodopsin in the Dark-Adapted State. *J. Mol. Biol.* **2005**, *352*, 319−328.
(18) Tsuda, M.; Ebrey, T. G. Effect of High Pressure on the Absorption Spectrum and Isomeric Composition of Bacteriorhodopsin. *Biophys. J.* **1980**, *30*, 149−157.
(19) Schulte, A.; Bradley, L., II. High-Pressure Near-Infrared Raman Spectroscopy of Bacteriorhodopsin Light to Dark Adaptation. *Biophys. J.* **1995**, *69*, 1554−1562.
(20) Bryl, K.; Yoshihara, K. Two Processes Lead to a Stable All-*trans* and 13-*cis* Isomer Equilibrium in Dark-Adapted Bacteriorhodopsin; Effect of High Pressure on Bacteriorhodopsin, Bacteriorhodopsin Mutant D96N and Fluoro-bacteriorhodopsin Analogues. *Eur. Biophys. J.* **2002**, *31*, 539−548.
(21) Seltzer, S. Solvent Isotope Effects on Retinal *Cis-Trans* Isomerization in the Dark Adaptation of Bacteriorhodopsin. *J. Am. Chem. Soc.* **1992**, *114*, 3516−3520.
(22) Neebe, M.; Rhinow, D.; Schromczyk, N.; Hampp, N. A. Thermochromism of Bacteriorhodopsin and Its pH Dependence. *J. Phys. Chem. B* **2008**, *112*, 6946−6951.
(23) Ludmann, K.; Gergely, C.; Váró, G. Kinetic and Thermodynamic Study of the Bacteriorhodopsin Photocycle over a Wide pH Range. *Biophys. J.* **1998**, *75*, 3110−3119.
(24) Váró, G.; Lanyi, J. K. Thermodynamics and Energy Coupling in the Bacteriorhodopsin Photocycle. *Biochemistry* **1991**, *30*, 5016−5022.
(25) Ghimire, G. D.; Sugiyama, H.; Sonoyama, M.; Mitaku, S. Regeneration of Bacteriorhodopsin from Thermally Unfolded Bacterio-Opsin and All-*trans* Retinal at High Temperatures. *Biosci. Biotechnol. Biochem.* **2005**, *69*, 252−254.
(26) Sonoyama, M.; Mitaku, S. High-Temperature Intermediate State of Bacteriorhodopsin Prior to the Premelting Transition of Purple Membrane Revealed by Reactivity with Hydrolysis Reagent Hydroxylamine. *J. Phys. Chem. B* **2004**, *108*, 19496−19500.
(27) Janovjak, H.; Kessler, M.; Oesterhelt, D.; Gaub, H.; Müller, D. J. Unfolding Pathways of Native Bacteriorhodopsin Depend on Temperature. *EMBO J.* **2003**, *22*, 5220−5229.
(28) Heyes, C. D.; El-Sayed, M. A. Thermal Properties of Bacteriorhodopsin. *J. Phys. Chem. B* **2003**, *107*, 12045−12053.
(29) Yokoyama, Y.; Sonoyama, M.; Mitaku, S. Inhomogeneous Stability of Bacteriorhodopsin in Purple Membrane against Photobleaching at High Temperature. *Proteins* **2004**, *54*, 442−454.
(30) Shnyrov, V. L.; Mateo, P. L. Thermal Transitions in the Purple Membrane from Halobacterium halobium. *FEBS Lett.* **1993**, *324*, 237−240.
(31) Wang, J.; El-Sayed, M. A. The Effect of Protein Conformation Change from α_{II} to α_{I} on the Bacteriorhodopsin Photocycle. *Biophys. J.* **2000**, *78*, 2031−2036.
(32) Wang, J.; El-Sayed, M. A. Temperature Jump-Induced Secondary Structural Change of the Membrane Protein Bacteriorhodopsin in the Premelting Temperature Region: A Nanosecond Time-Resolved Fourier Transform Infrared Study. *Biophys. J.* **1999**, *76*, 2777−2783.
(33) Hiraki, K.; Hamanaka, T.; Mitsui, T.; Kito, Y. Phase Transitions of the Purple Membrane and the Brown Holo-membrane X-ray Diffraction, Circular Dichroism Spectrum and Absorption Spectrum Studies. *Biochim. Biophys. Acta, Biomembr.* **1981**, *647*, 18−28.
(34) Oesterhelt, D.; Stoeckenius, W. Isolation of the Cell Membrane of Halobacterium halobium and Its Fractionation into Red and Purple Membrane. *Methods Enzymol.* **1974**, *31*, 667−678.
(35) Becher, B.; Tokunaga, F.; Ebrey, T. G. Ultraviolet and Visible Absorption Spectra of Purple Membrane Protein and Photocycle Intermediates. *Biochemistry* **1978**, *17*, 2293−2300.
(36) Cassim, J. Y. Unique Biphasic Band Shape of the Visible Circular Dichroism of Bacteriorhodopsin in Purple Membrane: Excitons, Multiple Transitions or Protein Heterogeneity? *Biophys. J.* **1992**, *63*, 1432−1442.
(37) Jackson, M. B.; Sturtevant, J. M. Phase Transitions of the Purple Membranes of Halobacterium halobium. *Biochemistry* **1978**, *17*, 911−915.
(38) Liu, J.; Liu, M. Y.; Nguyen, J. B.; Bhagat, A.; Mooney, V.; Yan, E. C. Y. Thermal Decay of Rhodopsin: Role of Hydrogen Bonds in Thermal Isomerization of 11-*cis* Retinal in the Binding Site and Hydrolysis of Protonated Schiff Base. *J. Am. Chem. Soc.* **2009**, *131*, 8750−8751.
(39) Liu, J.; Liu, M. Y.; Fu, L.; Zhu, G. A.; Yan, E. C. Y. Chemical Kinetic Analysis of Thermal Decay of Rhodopsin Reveals Unusual Energetics of Thermal Isomerization and Hydrolysis of Schiff Base. *J. Biol. Chem.* **2011**, *286*, 38408−38416.
(40) Schlebach, J. P.; Cao, Z.; Bowie, J. U.; Park, C. Revisiting the Folding Kinetics of Bacteriorhodopsin. *Protein Sci.* **2012**, *21*, 97−106.
(41) Ng, K. C.; Chu, L.-K. Effects of Surfactants on the Purple Membrane and Bacteriorhodopsin: Solubilization or Aggregation? *J. Phys. Chem. B* **2013**, *117*, 6241−6249.
(42) Tachikawa, H.; Iyama, T. TD-DFT Calculations of the Potential Energy Curves for the T*rans-Cis* Photo-isomerization of Protonated Schiff Base of Retinal. *J. Photochem. Photobiol. B* **2004**, *76*, 55−60.
(43) Humphrey, W.; Lu, H.; Logunov, I.; Werner, H.-J.; Schulten, K. Three Electronic State Model of the Primary Phototransformation of Bacteriorhodopsin. *Biophys. J.* **1998**, *75*, 1689−1699.

(44) Tallent, J. R.; Stuart, J. A.; Song, Q. W.; Schmidt, E. J.; Martin, C. H.; Birge, R. R. Photochemistry in Dried Polymer Films Incorporating the Deionized Blue Membrane Form of Bacteriorhodopsin. *Biophys. J.* **1998**, *75*, 1619−1634.
(45) Kubli-Garfias, C.; Salazar-Salinas, K.; Perez-Angel, E. C.; Seminario, J. M. Light Activation of the Isomerization and Deprotonation of the Protonated Schiff Base Retinal. *J. Mol. Model* **2011**, *17*, 2539−2547.
(46) Makhatadze, G. I.; Clore, G. M.; Gronenborn, A. M. Solvent Isotope Effect and Protein Stability. *Nat. Struct. Biol.* **1995**, *2*, 852−855.
(47) Makhatadze, G. I.; Privalov, P. L. Energetics of Protein Structure. *Adv. Protein Chem.* **1995**, *47*, 307−425.
(48) Garczarek, F.; Brown, L. S.; Lanyi, J. K.; Gerwert, K. Proton Binding within a Membrane Protein by a Protonated Water Cluster. *Proc. Natl. Acad. Sci. U. S. A.* **2005**, *102*, 3633−3638.
(49) Heyes, C. D.; Wang, J.; Sanii, L. S.; El-Sayed, M. A. Fourier Transform Infrared Study of the Effect of Different Cations on Bacteriorhodopsin Protein Thermal Stability. *Biophys. J.* **2002**, *82*, 1598−1606.
(50) Rothschild, K. J.; Clark, N. A. Polarized Infrared Spectroscopy of Oriented Purple Membrane. *Biophys. J.* **1979**, *25*, 473−487.
(51) Asai, M.; Tsuboi, M.; Shimanouchi, T.; Mizushima, S.-I. Infrared Spectra of Polypeptides and Related Compounds. I. *J. Phys. Chem.* **1955**, *59*, 322−325.
(52) Kim, J.; Schmitt, U. W.; Gruetzmacher, J. A.; Voth, G. A.; Scherer, N. E. The Vibrational Spectrum of the Hydrated Proton: Comparison of Experiment, Simulation, and Normal Mode Analysis. *J. Chem. Phys.* **2002**, *116*, 737−746.
(53) Garczarek, F.; Gerwert, K. Functional Waters in Intraprotein Proton Transfer Monitored by FTIR Difference Spectroscopy. *Nature* **2006**, *439*, 109−112.
(54) Groenendijk, G. W. T.; De Grip, W. J.; Daemen, F. J. M. Quantitative Determination of Retinals with Complete Retention of Their Geometric Configuration. *Biochim. Biophys. Acta* **1980**, *617*, 430−438.
(55) Oesterhelt, D.; Meentzen, M.; Schumann, L. Reversible Dissociation of the Purple Complex in Bacteriorhodopsin and Identification of 13-*cis* and All-*trans*-Retinal as its Chromophores. *Eur. J. Biochem.* **1973**, *40*, 453−463.